JACS
JOURNAL OF THE AMERICAN CHEMICAL SOCIETY

Communication

pubs.acs.org/JACS

Atomic Resolution Imaging of Grain Boundary Defects in Monolayer Chemical Vapor Deposition-Grown Hexagonal Boron Nitride

Ashley L. Gibb,[†,‡,§] Nasim Alem,[‡,§,∥] Jian-Hao Chen,[‡,§] Kristopher J. Erickson,[†,‡,§,#] Jim Ciston,[⊥] Abhay Gautam,[⊥] Martin Linck,[⊥,⊗] and Alex Zettl*[,‡,§]

Departments of [†]Chemistry and [‡]Physics, University of California, Berkeley, California 94720, United States
[§]Materials Sciences Division and [⊥]National Center for Electron Microscopy, Lawrence Berkeley National Laboratory, Berkeley, California 94720, United States

Supporting Information

ABSTRACT: Grain boundaries are observed and characterized in chemical vapor deposition-grown sheets of hexagonal boron nitride (h-BN) via ultra-high-resolution transmission electron microscopy at elevated temperature. Five- and seven-fold defects are readily observed along the grain boundary. Dynamics of strained regions and grain boundary defects are resolved. The defect structures and the resulting out-of-plane warping are consistent with recent theoretical model predictions for grain boundaries in h-BN.

Two-dimensional hexagonal nanomaterials such as graphene and hexagonal boron nitride (h-BN) have received significant research interest due to many unique properties.[1] Their sp^2-bonded character results in atomically thin films with excellent mechanical strength, chemical inertness, mechanical stability, and high thermal conductivity, as well as exciting electronic, optical, and magnetic properties.[2] Hexagonal boron nitride is isoelectronic with graphene, exhibiting the same sp^2 honeycomb structure, but is electronically insulating with a bandgap over 5 eV, suggesting a myriad of applications including coatings for aerospace technologies, high surface area materials for hydrogen storage, medicinal materials, and neutron shielding.[3,4] As a substrate for graphene, exfoliated h-BN has been shown to decrease charge density fluctuations and surface roughness, leading to greatly improved electronic properties.[5,6]

Although many exploratory fundamental studies can be performed with mechanically exfoliated h-BN or graphene, chemical vapor deposition (CVD)-synthesized materials are of particular interest due to their potential scalability. However, low and ambient pressure CVD synthesis routes on polycrystalline substrates lead to the presence of grain boundaries and other defects. A fundamental understanding of the interfaces between domains is critical for determining their effect on the mechanical, thermal, and electronic properties of these materials. Edge effects in particular are predicted to contribute to both electronic and magnetic edge-states.[7] Furthermore, the characterization and experimental control of these structures will be significant for any devices that contain them. The elucidation of the structure of CVD grown h-BN should be useful for informing synthetic approaches, similar to the recent progress of CVD grown graphene which was closely paired with detailed structural characterization. Prior work has determined the structure of vacancies, holes, line defects, and grain boundaries[8−10] in CVD graphene, as well as the structure of vacancy defects and holes in h-BN.[11] However, the structure of grain boundaries and many other defects in h-BN have not been investigated experimentally.

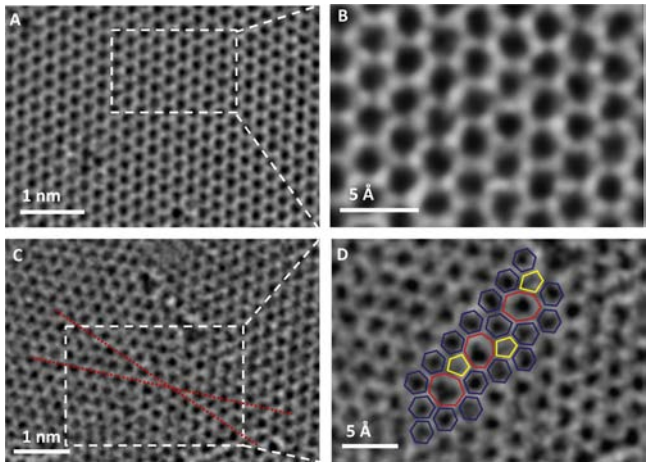

Figure 1. (A) HRTEM image of CVD-grown h-BN with (B) a magnified defect-free region. (C) Grain boundary in a monolayer of h-BN with a misorientation angle of 21°, and (D) magnified grain boundary defect structure from the inset. Hexagon, heptagon, and pentagon structures are depicted in blue, red, and yellow, respectively.

Recent theoretical calculations have been performed which motivate experimental verification of the h-BN grain boundary structure.[12] Work by Yakobson et al. indicates several possible structures for an h-BN grain boundary, and electronic calculations predict a change in band gap by as much as 38% owing to additional states along the boundary.[13] Similar to the modified electronic nature of graphene along its grain boundaries, this suggests the possibility of engineering grain boundaries to tailor material properties in h-BN.

In this paper we report the first transmission electron microscope investigation of CVD grown h-BN films with grain boundaries. Previous grain boundaries and other interfaces have been studied using scanning tunneling microscopy and low energy electron diffraction but their structure has not been resolved at the atomic scale.[14,15] In order to synthesize mono-

Received: January 19, 2013
Published: April 3, 2013

   dx.doi.org/10.1021/ja400637n | J. Am. Chem. Soc. 2013, 135, 6758−6761

and few-layer h-BN nanosheets, seen in Figure 1A, we used a low-pressure CVD approach, detailed in the Supporting Information. This allowed for the controllable growth of h-BN from solid, liquid or gaseous precursors including ammonia borane and borazine.[16,17] After synthesis, samples were analyzed via scanning electron microscopy and Raman spectroscopy, shown in Figures S1 and S2. These highly crystalline films preferentially grow on the surface of transition metal substrates such as nickel and copper.[18]

During CVD growth on the polycrystalline substrate, neighboring domains of misaligned orientations that originate from different nucleation points expand until they converge and form a grain boundary. These materials were then studied using transmission electron microscopy (TEM) with an *in situ* heating stage. To prepare the sample for TEM, the metal catalyst substrate was etched away using a solution of iron chloride. The film was then transferred to an *in situ* heating chip to allow for controlled Joule heating of the sample.[19] Sample architecture is shown in Figure S3.

TEAM 0.5, located at the National Center for Electron Microscopy at the Lawrence Berkeley National Laboratory was used for imaging at 80 kV, yielding a spatial resolution of about 1 Å. This resolution allows for atomic mapping of graphene or h-BN, but the signal-to-noise ratio was not sufficiently high to directly distinguish boron and nitrogen atoms in this experiment. During imaging, a monochromated electron beam was used to reduce the resolution-limiting effect of chromatic aberration. The spherical aberration was corrected to C3 = −8.2 μm in third order and C5 = 5.4 mm in fifth order. A small overfocus to compensate C3 and C5 allowed obtaining bright atom positions in the TEM images.[20] An *in situ* heating Aduro TEM holder (Protochips Inc.) was used to heat the sample from room temperature up to 800 °C within the TEM column during imaging.

During *in situ* heating, the stability and dynamics of defects, edges and the grain boundaries were investigated at atomic resolution. These dynamics reveal new defect structures not previously reported in h-BN. The sample was slowly heated to 800 °C to clean the sample and remove any remaining amorphous residues from the transfer step. Due to thermal and mechanical instabilities at 800 °C, the sample was cooled and high-resolution (HR) imaging was performed at 450 °C. At this temperature, moderate beam induced damage led to the formation of mono-vacancies but allowed imaging for ∼1 min before damage was critical enough to destroy a monolayer film.[21]

In Figure 1C, in a monolayer of h-BN, two domains with a misorientation angle of ∼21° meet to form a grain boundary. This grain boundary exhibits a structure which includes three pentagon−heptagon (5/7) defects as illustrated in Figure 1D. The observation of pentagon and heptagon structures might seem unexpected because an h-BN grain boundary with 5/7 defects will contain homonuclear boron−boron or nitrogen−nitrogen bonds. In a strictly planar configuration, boron−boron or nitrogen−nitrogen bonds are higher in energy than the heteronuclear boron−nitrogen bonds in the surrounding lattice.[13] However, under certain conditions, 5/7 defects are theoretically favored at h-BN grain boundaries,[13] as we discuss in more detail below. These structures will induce a local dipole moment at the grain boundary. Due to the structural orientation between multiple 5/7 defects in Figure 1D, if one contains a boron−boron bond, the other must contain a nitrogen−nitrogen bond, and thus these 5/7 features are of opposite polarities. A second grain boundary region, shown in Figure 2 also exhibits a similar 5/7 defect structure, again with bond orientations between the pentagon-heptagon defects indicating homonuclear bonds of opposite polarity, i.e., B−B and N−N. The fast Fourier transforms (FFTs) in Figure 2A obtained from the two sides of the grain boundary indicate a ∼22° angle, comparable to the angle in Figure 1.

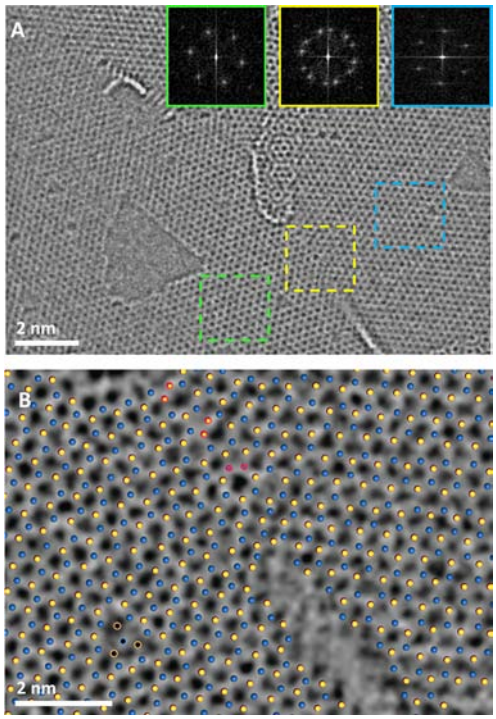

Figure 2. (A) HRTEM image of a monolayer h-BN film with a grain boundary. Insets are fast Fourier transforms from regions on the left (green), on the right (blue), and in the middle (yellow) of the grain boundary, displaying lattice misorientation. (B) Atomically mapped grain boundary from the boron nitride lattice in (A). Blue spheres are nitrogen, yellow spheres are boron, and red indicates locations of possible homonuclear bonds. Black filled spheres are vacancy defects.

In order to clarify the bonding at the grain boundaries, atoms were mapped up to the grain boundary as shown in Figure 2B. While it was not feasible to experimentally determine the elemental identity of single atoms at the grain boundary in this experiment, analysis of knock-on damage in the lattice helps to elucidate possible atomic configurations. Previous work has shown that beam damage at an accelerating voltage of 80 kV more heavily impacts just one sublattice (either B or N), causing mono-vacancy formation in one sublattice of monolayer h-BN, which is followed by Sierpinski triangle-like growth of vacancies into larger holes.[22] Additional work found that these mono-vacancies were primarily formed as a result of an ejected boron atom, due to the lower knock on energy threshold of boron.[11,23,24] In Figure 2B, boron and nitrogen atoms were identified by assigning isolated mono-vacancies as missing boron atoms and confirming this at larger defects, which will have primarily nitrogen terminated edges, consistent with previous work. The bond energies and knock-on energy thresholds at the grain boundaries may differ from the bulk, so mono-vacancies close to, but not at, the grain boundary were chosen. Based on the atomic structure in Figure 2B, we predict that if this grain boundary consists purely of only boron and nitrogen atoms it will contain three homonuclear bonds: two boron−boron bonds and one nitrogen−nitrogen bond.

dx.doi.org/10.1021/ja400637n | J. Am. Chem. Soc. 2013, 135, 6758−6761

A comparison with other stoichiometric boron and nitrogen containing structures, such as boron nitride nanotubes (BNNTs) provides insight into such defect structures. Research shows defect structures such as 5/7- or 4/8-membered rings form at the closed ends of BNNTs.[25] The two main factors that affect the preference of either 4/8 or 5/7 defects are mechanical strain and chemical stability.[26] While 5/7 rings necessitate higher energy homonuclear bonds, in a heteronuclear bonded 4/8 defect the rings will be highly strained and will likely exhibit significant out of plane local bending of the membrane. From experimentally observed angles and structural geometry of BNNTs, past researchers have suggested that BNNTs contain square−octagon (4/8) defect structures.[27] If a similar structure holds for sheets of boron nitride, these same 4/8 defects might be expected at strained grain boundaries and interfaces.

Recent theoretical calculations of the energies of 5/7 and 4/8 defect structures in h-BN sheets has predicted that both possible defect structures are within reasonable energy ranges, especially with high local strain, such as long-range curvature perpendicular to the lattice.[13] Those calculations found that constraining the lattice to a two-dimensional plane will lead to 5/7 defects at dislocation cores with energy ∼6 eV less than a 4/8 defect, but the introduction of curvature in the sheet favors the 4/8 structure by 1 eV.

While the 5/7 rings in Figure 1 exist in a region of the lattice that appears flat, the grains often appear to be under strain or contain three-dimensional warping along the grain boundary in the form of a wrinkle protruding normal to the lattice plane. This can be seen in the lower right corner of Figure 2A, with a second grain boundary region imaged near several triangular holes and monovacancies. Similar to graphene, boron nitride has a negative coefficient of thermal expansion, which causes the film to stretch when cooled. Conversely, the underlying support will shrink while cooled, resulting in the formation of wrinkles. Time series images in Figure 3 show that this warped structure is dynamic and eventually flattens, introducing additional in-plane strain in the unit cells around the grain boundary. This strain may affect the geometry of the grain boundary and which local structures will be preferred, as explained by Yakobson et al., who predicted

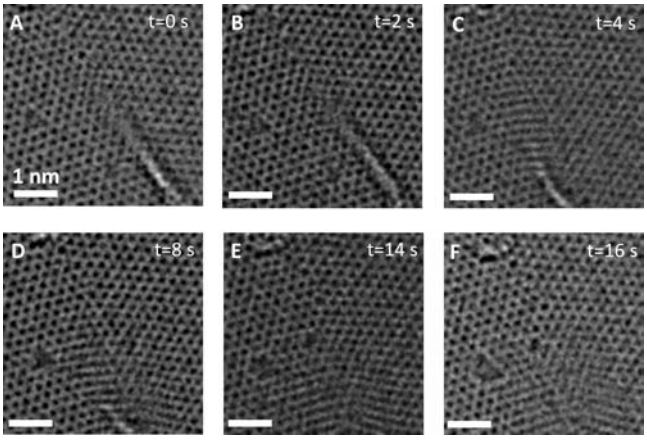

Figure 3. HRTEM time series images of a grain boundary in a h-BN film. (A) Out-of-plane strain and warping is visible in the lower right corner and has dynamic behavior. (B) After 2 s the wrinkle remains but the local structure of the 5/7 defects have changed. The wrinkle translates and has changed curvature after 4 s (C), before flattening into the plane of the film at 8 s (D), thereby forming a strained nanograin at 14 s (E) and 16 s (F). Scale bars, 1 nm.

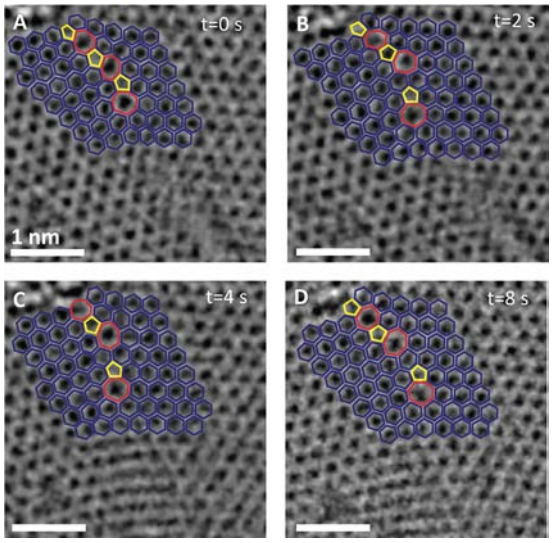

Figure 4. (A) HRTEM image of a grain boundary in a boron nitride film with three 5/7 defects. (B) After 2 s, one 5/7 pair has migrated by one unit cell. (C) After 4 s, the 5/7 defects remain in place, but the out-of-plane warping has changed. (D) After 8 s, the lower Stone−Wales-like defect has again migrated by a single unit cell. Scale bars, 1 nm.

that 5/7 h-BN grain boundaries would relax to have inflection angles of up to 53°, with their 4/8 counterparts at as high as 77°.[13] Other work has shown that localized out of plane bending occurs at mono-vacancies in order to relax a defect in h-BN.[28]

Although vacancies, larger defects, and wrinkles with high local strain exist along the grain boundary and were dynamic, we found that the boundary itself was robust under e-beam irradiation at 80 kV. In our experiment, we observed that over a period of 16 s the inflection angle changed, and the boundary relaxed from the highly strained wrinkle in Figure 3A to the planar structure shown in Figure 3F. During the relaxation of the wrinkle, a nanograin formed, resulting in a change in the grain boundary tilt angle. In Figure 3F the grain boundary angle varies by as much as 4° over a planar distance of 2 nm due to strain relaxation in the lattice.

In addition to the change in inflection angle, the 5/7 defects migrated apart by one unit cell over 4 s (Figure 4A−C), and again after 8 s (Figure 4D), but otherwise remained stable under the electron beam and applied heat. This migration accompanied the inflection angle strain relaxation. The migration could be caused by defect−defect repulsion between 5/7 defects of different orientations. Another possibility for the formation and migration of the 5/7 structures observed above could be the incorporation of dopant atoms into the boron nitride lattice at the grain boundary. Although we were careful to prevent contamination during the synthesis, prior work has shown that amorphous carbon and other contaminants tend to accumulate along grain boundaries in graphene. Additionally, carbon and oxygen point defects have been observed in a boron nitride lattice.[29]

Available theoretical studies of grain boundaries in h-BN consider strictly boron and nitrogen atomic constituents, with predictions in excellent agreement with experimental observations presented here for nominally pure h-BN. It would be interesting to extend theoretical models to include substitutional impurities, notably carbon. Temperature-derived energetics of B−B, N−N, and B−C−N bonds and 5/7 rings made of those two or three species may be rather different. Intriguing would be experimental studies on intentionally doped h-BN, for example

dx.doi.org/10.1021/ja400637n | J. Am. Chem. Soc. 2013, 135, 6758−6761

with carbon or oxygen. Structural analysis of intentionally doped $B_xC_yN_z$ samples suggest that during growth the materials usually phase segregate into patches of pure carbon (graphene) and pure h-BN;[30] the grain boundary structure in these inhomogeneous materials is unknown.[31]

Future experiments using EELS, annular dark-field TEM, and ADF-STEM[29,32] would be helpful to explore the properties of h-BN and to further clarify the atomic structure under different doping conditions. Unfortunately, the powerful atomic identification STEM methods applied previously to h-BN and other materials are difficult to apply to the grain boundary regions in h-BN. We have found that the atoms in regions surrounding defects are less stable than those of the ideally bonded bulk, and these instabilities greatly complicate data collection and analysis.

The unusual atomic arrangements at h-BN grain boundaries are expected to lead to a host of new materials properties, including modified electronic bandgap,[13,33] new chemical reactivity, and altered mechanical properties. These features might be favorably exploited in "tuning" BN for specific applications.[34,35]

In conclusion, we report the first atomic resolution TEM images of grain boundaries in a hexagonal boron nitride lattice. These grain boundaries indicate novel dynamic defect structures that have not been previously observed in h-BN.

■ ASSOCIATED CONTENT

Supporting Information

Sythesis details, sample schematic, Raman data, imaging conditions, and processing information. This material is available free of charge via the Internet at http://pubs.acs.org.

■ AUTHOR INFORMATION

Corresponding Author

azettl@physics.berkeley.edu

Present Addresses

[‖]N.A.: Pennsylvania State University, University Park, PA
[#]K.J.E.: Sandia National Laboratory, Livermore, CA
[⊗]M.L.: CEOS GmbH, Heidelberg, Germany

Notes

The authors declare no competing financial interest.

■ ACKNOWLEDGMENTS

This work was supported in part by the Director, Office of Energy Research, Office of Basic Energy Sciences, Materials Sciences and Engineering Division, of the U.S. Department of Energy under Contract #DE-AC02-05CH11231 which provided for detailed TEAM imaging at the National Center for Electron Microscopy; the Office of Naval Research under MURI award N00014-09-1-1066 which provided for postdoctoral support for image analysis; and the Air Force Office of Scientific Research under grant #FA9950-10-1-0451 which provided for hBN synthesis. AG acknowledges support from an NSF graduate research fellowship.

■ REFERENCES

(1) Geim, A. K.; Novoselov, K. S. *Nat. Mater.* **2007**, *6*, 183.
(2) Rao, C. N. R.; Sood, A. K.; Subrahmanyam, K. S.; Govindaraj, A. *Angew. Chem., Int. Ed.* **2009**, *48*, 7752.
(3) Pacilé, D.; Meyer, J. C.; Girit, C. O.; Zettl, A. *Appl. Phys. Lett.* **2008**, *92*, 133107.
(4) Golberg, D.; Bando, Y.; Huang, Y.; Terao, T.; Mitome, M.; Tang, C. *ACS Nano* **2010**, *4*, 2979.
(5) Wang, Y.; Brar, V. W.; Regan, W.; Tsai, H.; Wu, Q.; Gannett, W.; Zettl, A.; Crommie, M. F. *Nano Lett.* **2011**, 2291.
(6) Gannett, W.; Regan, W.; Watanabe, K.; Taniguchi, T.; Crommie, M. F.; Zettl, A. *Appl. Phys. Lett.* **2011**, *98*, 242105.
(7) Topsakal, M.; Akrurk, E.; Ciraci, S. *Phys. Rev. B* **2009**, *79*, 115442.
(8) Kim, K.; Lee, Z.; Regan, W.; Kisielowski, C.; Crommie, M. F.; Zettl, A. *ACS Nano* **2011**, *5*, 2142.
(9) Huang, P. Y.; Ruiz-Vargas, C. S.; van der Zande, A. M.; Whitney, W. S.; Levendorf, M. P.; Kevek, J. W.; Garg, S.; Alden, J. S.; Hustedt, C. J.; Zhu, Y.; Park, J.; McEuen, P. L.; Muller, D. A. *Nature* **2011**, *469*, 389.
(10) Wei, Y.; Wu, J.; Yin, H.; Shi, X.; Yang, R.; Dresselhaus, M. *Nat. Mater.* **2012**, *11*, 759.
(11) Alem, N.; Erni, R.; Kisielowski, C.; Rossell, M.; Gannett, W.; Zettl, A. *Phys. Rev. B* **2009**, *80*, 155425.
(12) Wang, Z. *J. Nanopart. Res.* **2012**, *14*, 756.
(13) Liu, Y.; Zou, X.; Yakobson, B. I. *ACS Nano* **2012**, *6*, 7053.
(14) Auwärter, W.; Muntwiler, M.; Osterwalder, J.; Greber, T. *Surf. Sci.* **2003**, *545*, 735.
(15) Joshi, S.; Ecija, D.; Koitz, R.; Iannuzzi, M.; Seitsonen, A. P.; Hutter, J.; Sachdev, H.; Vijayaraghavan, S.; Bischoff, F.; Seufert, K.; Barth, J. V; Auwärter, W. *Nano Lett.* **2012**, *12*, 5821.
(16) Kim, K. K.; Hsu, A.; Jia, X.; Kim, S. M.; Shi, Y.; Dresselhaus, M.; Palacios, T.; Kong, J. *ACS Nano* **2012**, *6*, 8583.
(17) Song, L.; Ci, L.; Lu, H.; Sorokin, P. B.; Jin, C.; Ni, J.; Kvashnin, A. G.; Kvashnin, D. G.; Lou, J.; Yakobson, B. I.; Ajayan, P. M. *Nano Lett.* **2010**, *10*, 3209.
(18) Kim, K. K.; Hsu, A.; Jia, X.; Kim, S. M.; Shi, Y.; Hofmann, M.; Nezich, D.; Rodriguez-Nieva, J. F.; Dresselhaus, M.; Palacios, T.; Kong, J. *Nano Lett.* **2012**, *12*, 161.
(19) Ismach, A.; Chou, H.; Ferrer, D. A.; Wu, Y.; McDonnell, S.; Floresca, H. C.; Covacevich, A.; Pope, C.; Piner, R.; Kim, M. J.; Wallace, R. M.; Colombo, L.; Ruoff, R. S. *ACS Nano* **2012**, *6*, 6378.
(20) Lentzen, M. *Microsc. Microanal.* **2008**, *14*, 16.
(21) Kotakoski, J.; Jin, C.; Lehtinen, O.; Suenaga, K.; Krasheninnikov, A. *Phys. Rev. B* **2010**, *82*, 1.
(22) Meyer, J. C.; Chuvilin, A.; Algara-Siller, G.; Biskupek, J.; Kaiser, U. *Nano Lett.* **2009**, *9*, 2683.
(23) Alem, N.; Erni, R.; Kisielowski, C.; Rossell, M. D.; Hartel, P.; Jiang, B.; Gannett, W.; Zettl, A. *Phys. Status Solidi RRL* **2011**, *5*, 295.
(24) Zobelli, A.; Gloter, A.; Ewels, C.; Seifert, G.; Colliex, C. *Phys. Rev. B* **2007**, *75*, 245402.
(25) Saito, Y.; Maida, M. *J. Phys. Chem. A* **1999**, *103*, 1291−1293.
(26) Rogers, K. M.; Fowler, P. W.; Seifert, G. *Chem. Phys. Lett.* **2000**, *332*, 43.
(27) Bengu, E.; Marks, L. *Phys. Rev. Lett.* **2001**, *86*, 2385−2387.
(28) Alem, N.; Yazyev, O.; Kisielowski, C.; Denes, P.; Dahmen, U.; Hartel, P.; Haider, M.; Bischoff, M.; Jiang, B.; Louie, S.; Zettl, A. *Phys. Rev. Lett.* **2011**, *106*, 126102.
(29) Krivanek, O. L.; Chisholm, M. F.; Nicolosi, V.; Pennycook, T. J.; Corbin, G. J.; Dellby, N.; Murfitt, M. F.; Own, C. S.; Szilagyi, Z. S.; Oxley, M. P.; Pantelides, S. T.; Pennycook, S. J. *Nature* **2010**, *464*, 571.
(30) Ci, L.; Song, L.; Jin, C. H.; Jariwala, D.; Wu, D. X. J.; Li, Y. J.; Srivastava, A.; Wang, Z. F.; Storr, K.; Balicas, L.; Liu, F.; Ajayan, P. F. *Nat. Mater.* **2010**, *9*, 430.
(31) Sutter, P.; Cortes, R.; Lahiri, J.; Sutter, E. *Nano Lett.* **2012**, *12*, 4869.
(32) Krivanek, O. L.; Dellby, N.; Murfitt, M. F.; Chisholm, M. F.; Pennycook, T. J.; Suenaga, K.; Nicolosi, V. *Ultramicroscopy* **2010**, *110*, 935.
(33) Jung, J.; Qiao, Z.; Niu, Q.; Macdonald, A. H. *Nano Lett.* **2012**, *12*, 2936.
(34) Levendorf, M. P.; Kim, C. J.; Brown, L.; Huang, P. Y.; Havener, R. W.; Muller, D. A.; Park, J. *Nature* **2012**, *488*, 627.
(35) Tsen, A. W.; Brown, L.; Levendorf, M. P.; Ghahari, F.; Huang, P. Y.; Ruiz-Vargas, S.; Havener, R. W.; Muller, D. A.; Kim, P.; Park, J. *Science* **2012**, *336*, 1143.